

# Petrology and Geochemical Characteristics of Penja Migmatites in the Cameroon Pan-African Fold Belt

Ndema Mbongué Jean-Lavenir

**Abstract** — Penja migmatites are situated within the central domain of the Pan-African fold belt in Cameroon. They occur as a large migmatitic gneiss body and comprise migmatitic biotite-gneisses, migmatitic mylonitic gneisses, amphibolites and granite pegmatites. Field observations and petrography results favour a melting process and Penja migmatites range from metatexite to diatexite related to the amphibolite facies. Penja migmatites display three types of neosome: leucosome, melanosome and mesosome; these neosomes are interpreted as the result of incipient migmatization of the gneiss. The presence of neosome suggests a high rheological contrast between the neosomes and the surrounding gneiss. The proportion of neosome varies between 20 to 50% and it segregated into leucosome and melanosome. Penja migmatites fall into the group of gneissic granitic rock, stromatic structures and granoblastic microstructures prevail in the rock types, mylonitic microstructures are also recorded. Three types of leucosomes such as leucosome dike, in situ leucosome and in-source leucosome are recognized in the Penja migmatites and the difference between the three types could be linked to the difference in the composition of their source and the probable contamination during transportation of the melting material. The partial melting constitutes the mechanism in the formation of Penja migmatites and therefore the migmatite rock of Penja refers to venite. Penja migmatite rocks exhibit the composition of intermediate to acid High-K calc-alkaline series and I-type rocks derived from continental igneous protoliths varying from granites, diorite quartzite and granodiorite. The rare earth elements and multi-element patterns are in accordance with genetic processes involving participation of the crust.

**Key words** — Penja migmatites, Metatexites to diatexite, Neosome, Gneissic granitic rock, Venite, High-K calc-alkaline series

## 1 INTRODUCTION

The term migmatite was introduced by [1] for gneisses composed of two genetically different components, one of which was a schistose sediment or foliated eruptive and the other formed by resolution of material like the first or by an injection from without. Mehnert (1968) proposed a much less restrictive and nongenetic definition: a migmatite is a megascopically composite rock consisting of two or more petrographically different parts, one of which is the country rock in a more or less metamorphic stage, the other is of pegmatitic, aplitic, granitic or generally plutonic appearance. Therefore, a migmatite refer to a rock that is a mixture of metamorphic rock and igneous rock (intrusive rock). It is created when a metamorphic rock such as gneiss partially melts, and that melt recrystallizes into an igneous rock, creating a mixture of the unmelted metamorphic part with the recrystallized igneous part.

According to [3], the migmatite group includes gneissic granitic rocks frequently blind-ending veins, breccias-like

granites with innumerable fragments of more or less completely dissolved older rocks, and some striped granites in which only the still preserved parallel structure indicates a faint remnant of the original properties of the rock.

Migmatites form under extreme temperature conditions during prograde metamorphism, where partial melting occurs in pre-existing rocks. They are not crystallized from a totally molten material, and are not generally the result of solid-state reactions.

The IUGS Subcommission on the Systematic of Metamorphic Rocks [4] and definition of [5] has described two bases for the assessment of migmatites: (1) the relative age of the components and (2) the colour index. Neosome and paleosome define the elements on the basis of relative ages. Neosome is the newly formed parts of a migmatite which can range from leucocratic to melanocratic in colour while paleosome represents the relict part from the parent rock from which the migmatite is generated. Partial melting is the focal process in the generation of neosome and its components.

Based on the colour index of the neosome, three main types of neosome can be identified [3], [6]: (i) leucocratic usually rich in quartz and feldspars and designated as the leucosome (lightest part of migmatite), (ii) The melanosome is enriched in dark, mafic minerals, mostly biotite and amphibole and (iii) the mesosome is developed of non-segregated partial melt (magma) which is intermediate between leucosome and melanosome. Sometimes mesosome has been defined as a synonym for paleosome [3]. The aim of this work is to determine the origin and evolution of the formation of the Penja

*Department of Geology, University of Buea, P.o. Box 63, Buea, South West Region, Cameroon.*

*Laboratory of Petrology and Structural Geology, Department of Earth Sciences, Faculty of Sciences, University of Yaoundé I, Cameroon.*

E-mail : [jndema2012@gmail.com](mailto:jndema2012@gmail.com)

migmatite rocks situated in the central domain of the Cameroon Pan-African Fold Belt.

## 2 GEOLOGICAL SETTING

Penja migmatites (PMs) are located in the southwestern part of the central domain of the Pan-African Fold Belt (PAFB) in Cameroon (Fig.1). The PAFB or Central African Orogen (CAO) is a major Neoproterozoic Orogen linked to the Trans-Saharan Belt of western Africa and to the Brasiliano Orogen (BO) of NE Brazil [7], [8]. In Cameroon, three main domains were distinguished in the Pan-African Central Africa Fold Belt [9] - [15]. These are from south to north (Fig. 1): (1) the southern domain, which corresponds to the northern edge of the Congo Craton, formed by Neoproterozoic metasediments deposited in a passive margin environment and metamorphosed under high pressure conditions at 616 Ma; (2) the northern domain consisting of subordinate 830 Ma old metavolcanic rocks of tholeiitic and alkaline affinities; (3) the central domain, which

contains the present study area, is situated between the Sana-ga shear zone (SSZ) and the Betaré-Oya shear zone (BOSZ; [18] to the south, and the Tibati-Banyo fault (TBSZ) to the north [19]). The central Cameroon domain is dominated by a NE-SW elongated regional-scale plutonic complex intrusive into a Paleoproterozoic basement and locally covered by Cretaceous deposits (Mbere and Djerem basins) and by Cenozoic volcanic rocks of the Cameroon Volcanic Line (CVL). Penja is located between latitude 4°37'-4°40' Nord and between longitude 9°40'-9°42' East and belongs to the southwest sector of the Tombel graben and constitute a sequence of the Tombel Shear Zone (TSZ) which is a segment of the Central Cameroon Shear Zone (CCSZ).

## 3 ANALYTICAL METHODS

Fresh rock samples were collected and more than twelve thin sections were prepared at the University of Yaoundé I for petrographic studies. Detailed descriptions of thin sections were done using conventional techniques at the University of Buea, Cameroon. Mineral abbreviations recommendations by the IUGS Subcommittee on the Systematics of Metamorphic Rocks are according to [20]. Eleven representative samples were selected for chemical analysis using the pulp. Whole rock geochemical composition was obtained by Inductively Coupled Plasma-Optical Emission Spectrometry (ICP-OES) for major elements, beryllium (Be) and scandium (Sc), and by Inductively Coupled-Plasma Mass Spectrometry (ICP-MS) for trace elements and rare earth elements (REE) at Activation Laboratories (ACTLABS) in Canada. The samples were pulverized to obtain a homogeneous sample out of which 0.2 g of rock powder was fused with 0.9g lithium metaborate/tetraborate at 1000°C, and then dissolved in 100 mm<sup>3</sup> of HNO<sub>3</sub> at 4%. The fusion ensures that the entire sample is dissolved. It is only with this attack that major oxides including SiO<sub>2</sub>, refractory minerals (zircon, sphene, monazite, chromite, gahnite), REE and other high field strength elements (HFSE) are put into solution. Analytical uncertainties vary from 0.1 to 0.04% for major elements, 0.1 to 0.5% for trace elements, 0.01 to 0.5 ppm for REE, and total includes all elements in % oxide. To test for analytical precision, duplicate samples chosen from the batch were randomly placed in each analysis. Loss on ignition (LOI) was determined by gravimetry. Different standards and typical detection limits were used; data quality assurance was established by applying these standards as unknown between samples.

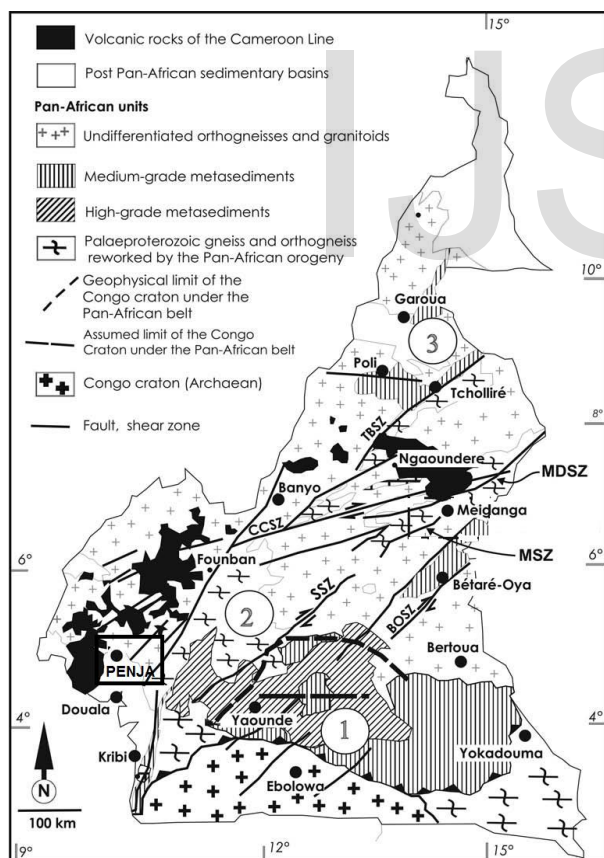


**Fig.1:** Geological map of Cameroon (modified from [10], [14], [16] - [18], showing major lithotectonic units and shear zones: (1) southern domain; (2) central domain; (3) northern domain; CCSZ, Central Cameroon shear zone; TBSZ, Tcholliré-Banyo shear zone; SSZ, Sanaga shear zone; BOSZ, Betaré- Oya shear zone. The location of the study area Penja in the central Cameroon is marked by a box.

## 4 RESULTS

### 4.1 Petrography

Penja migmatites (PMs) occur as a large body with a dome-shaped as isolated outcrops of migmatitic gneisses located at the northern end of Penja and comprising many rock types such as migmatitic biotite-gneisses, migmatitic mylonitic gneisses, amphibolites and some granite pegmatites.

Migmatitic biotite-gneisses (Fig. 2a) are the main rock type; they are light to dark-grey in colour and show medium to coarse grained (average grain size 0.5 cm), displaying a millimetric to centimetric compositional layering with alternating ferromagnesian-rich bands and quartzo-feldspathic layers. They display granoblastic microstructures (Fig. 2b), mainly composed of biotite (20-25%), hornblende (5%), plagioclase (18-20%), quartz (20-25%), K-feldspar (Kfs) include orthoclase (8%) and microcline (10-13%). Accessory minerals consist of opaque oxides and represent 2%. Structurally, migmatitic biotite-gneisses show a regional-scale mylonitic foliation  $S_1$  underlined by stretched quartz, preferred orientation of quartz ribbons and biotite lamellae. This foliation is associated with the first phase of deformation  $D_1$ . The migmatitic biotite-gneisses display an amphibolite facies assemblage: Hbl + Bt + Pl + Qtz + Kfs + Op. This assemblage is contemporaneous with  $D_1$  deformation and characterized by a mylonitic foliation  $S_1$  generally oriented in the N-S and NNE-SSW direction.

Migmatitic mylonitic gneisses (Fig. 2c) are either fine to medium-grained or either medium to coarse grained massive rock. Augen or mylonitic microstructures prevail in these rocks. They display quartzo-feldspathic and ferromagnesian segregation characterized by alternating of light and dark bands. The thicknesses of the light bands vary from millimeters to centimeters while dark bands are millimetric. Under the microscope (Fig. 2d), the light bands contain minerals such as quartz (25-28%), microcline (15-20%) and plagioclase (10-15%); the dark bands are rich in ferromagnesian minerals such as biotite (15-20%) and hornblende (10%). Accessory phases (3%) are opaque oxides. The rock exhibits a pronounced mylonitic foliation  $S_1$  outlined by the preferred orientation of quartz ribbons and biotite lamellae, stretched quartz, aggregate of quartz, sigmoid and lens-shaped quartz and feldspar. Light bands are more abundant due to the migmatization. The amphibolite facies assemblage observed in this rock type is Bt + Pl + Qtz + Mc + Hbl + Op, also characterized by a mylonitic foliation  $S_1$ .

Amphibolites (Fig. 2e) are dark in colour, they consist of fine grained rocks and occur as relicts. Under the microscope they display a granoblastic microstructure (Fig. 2f) composed

of hornblende (30-35%), biotite (10-20%), quartz (10-15%) and feldspar (10-15%), orthoclase (4%) and microcline (7%). Opaque oxides (3%) occur as accessory phases. Amphibolites also display an amphibolite facies assemblage underlined by Hbl + Bt + Pl + Qtz + Mc + Or + Op.

Granite pegmatites (Fig. 2g) are syn-metamorphic and occur along the shear zones. This rock type is light in colour and displays very coarse-grained having a grain size of 3 cm or larger with interlocking crystals. They show pegmatitic texture (Fig. 2h) composed of quartz (35-38%), microcline (20-25%), plagioclase (25-30%) and shiny flakes of biotite (3-5%). Accessory minerals such as opaque oxides represent about 2%.

### 4.2 Characteristic Elements of Penja Migmatites

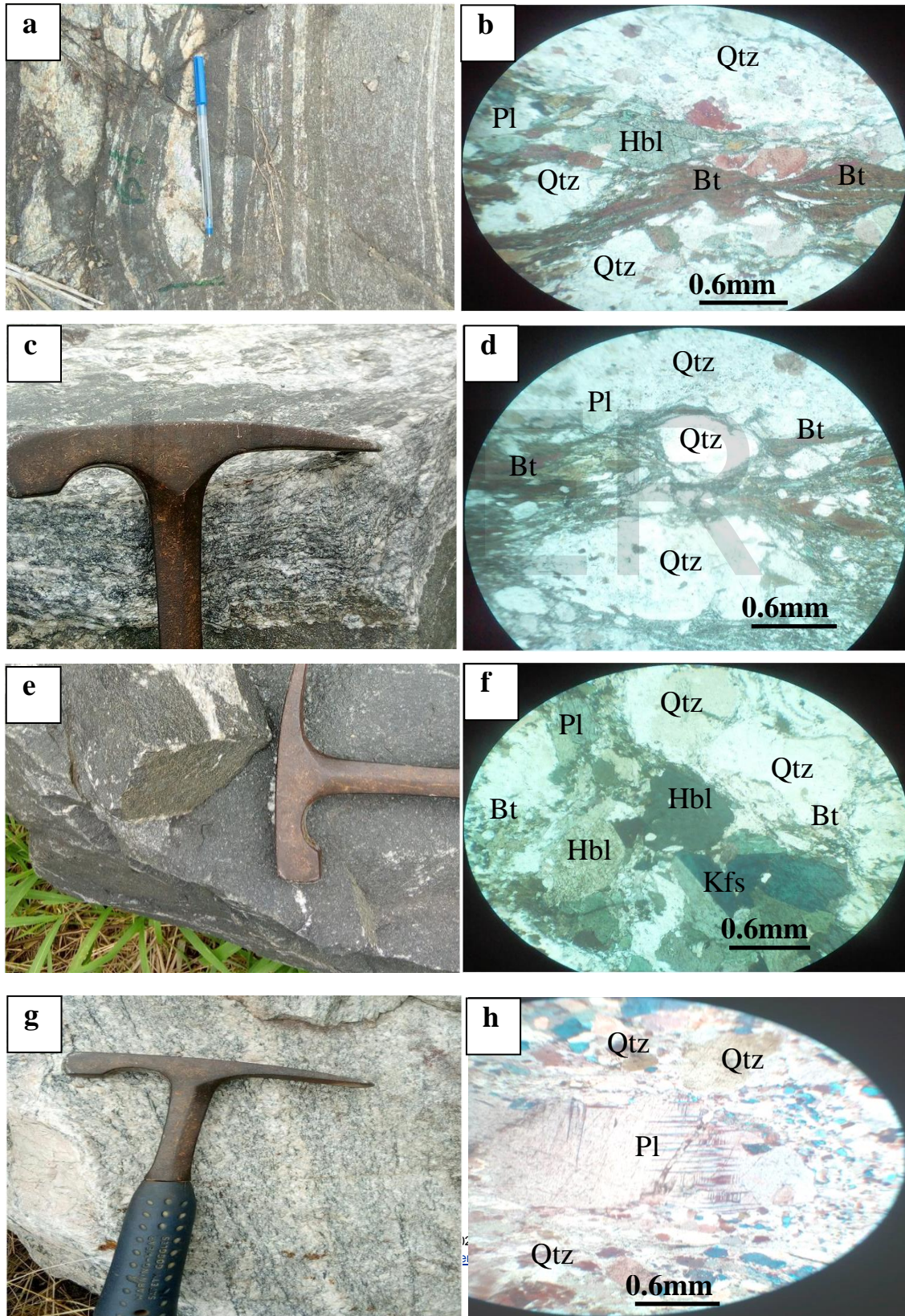
In the PMs, the quartzo-feldspathic fraction and related dark ferromagnesian minerals are the most frequently intimately associated although dark selvages are seldomly observed. The neosome is segregated into leucosome and melanosome and its proportion range from 20 to 50%. On the basis of field observations and the colour index of neosome, the study area experienced three types of neosome: leucosome or leucocratic neosome, melanosome and mesosome (Fig. 3a); also the neosome and mesosome have a layered structure (Fig. 2a, 3a).

Leucosome refers to the lightest part or the lightest type of neosome; three types of leucosomes were recognized in the study area: leucocratic dike (or leucosome dike), in situ leucosome and in-source leucosome. Leucosome dikes are the most abundant in the Penja migmatitic gneisses. They occur as single dykes (Fig. 3b) and as conjugated dikes (Fig. 3c). Leucosome dikes are fine-grained, composed of ribbons or interstitial quartz (45-50%), feldspar (30-35% crystals and associated ferromagnesian minerals (< 5%). In situ leucosomes (Fig. 3d, 3e) are structured or not and occur along the ductile shear zones. They exhibit medium to coarse-grained (average grain size = 4 mm), large bands of 5 to 20 cm thick. In situ leucosomes contain quartz (35-40%), feldspar (30-35%), and related mafic minerals (< 15%). Quartz forms either elongated and interstitial crystals or either almond-shaped and sigmoid-shaped. In-source leucosome (Fig. 3f) are coarse grained and occur along ductile shear zones, shear band cleavages and are also found in the pressure shadows of the basic pods minerals. They are composed of ribbons and interstitial quartz (35-45%), feldspar (30-40%) and related ferromagnesian minerals (< 5%).

Melanosome is made up of mafic minerals and occurs as intermediate part ferromagnesian-rich mineral or dark millimetric to centimetric bands. It is composed of biotite (30-40%), amphibole (45-50%) and sometime few interstitial quartz and feldspar in very minor percentage (Fig. 3a, 3g).

Mesosome or paleosome (Fig. 3g) occurs as dark lens (with variable sizes) composed of relict of amphibolites. The mesosome represents the residue of the melt. The paleosome is not affected by partial melting, and in which features older than the partial melting (layering, foliation, folding) have been preserved (Fig. 3g).

Fig. 2 : Macrophotograph and microphotograph for the various rock types



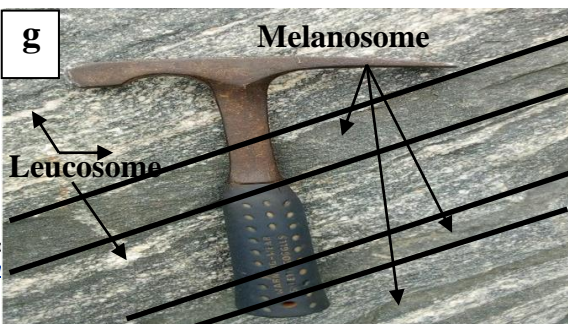
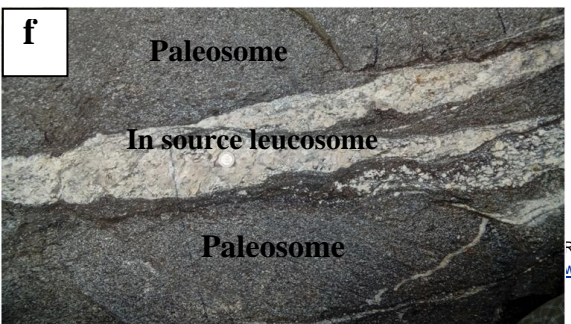
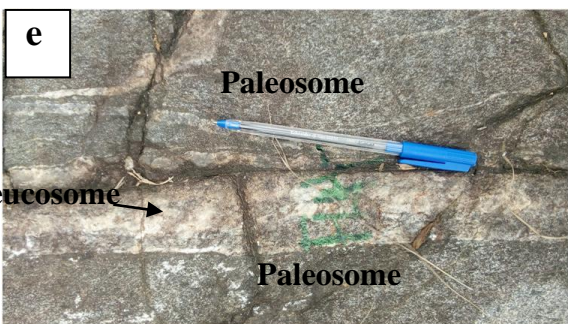
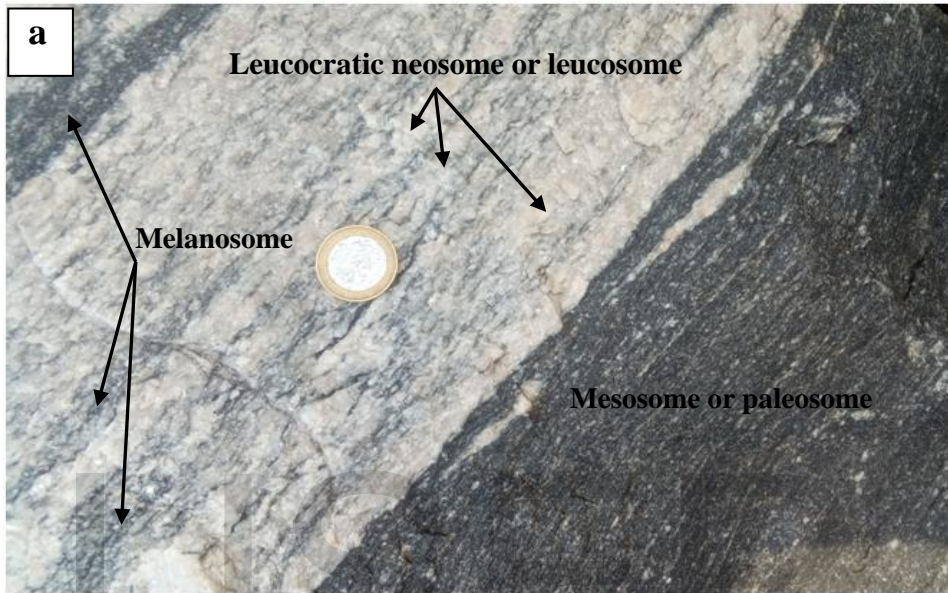


**Fig. 3:** (a) = Various aspect of neosome in the Penja migmatites, note the layered structure of neosome and mesosome; (b) to (g) = Field occurrence of leucosome, melanosome and paleosome.

IJSER

### 4.3 Whole Rock Geochemical Characteristics

The chemical composition of PMs is presented in table 1. After plotting geochemical data bases of the samples on  $\text{Fe}_2\text{O}_3 + \text{TiO}_2 + \text{CaO}$  vs.  $\text{Al}_2\text{O}_3$  whole rock diagram of [21] represented in figure 4a, the samples define a chemical trend parallel to the igneous rocks origin, and their protoliths have ranged from granite to diorite quartzite (quartz diorite) through granodiorite. Migmatitic biotite-gneisses and migmatitic mylonitic gneisses have the composition of granite (Fig. 4a). These two rock types are silica-rich rocks with a total range of 68.68 to 69.49%  $\text{SiO}_2$  in migmatitic biotite-gneisses and 73.65 to 75.13%  $\text{SiO}_2$  in migmatitic mylonitic gneisses (Table 1), and they fall into the group of acid rocks. Amphibolites exhibit a chemical composition of granodiorite and diorite quartzite (Fig. 4a) and yields in the group of intermediate rocks with  $\text{SiO}_2$  concentration ranging from 55.33-60.67% (Table 1). Based on the diagram of  $\text{SiO}_2$  vs.  $\text{K}_2\text{O}$  [22], all the rock types have been set to High-K calc-alkaline series (Fig. 4b); sample PJ4 of amphibolites and sample PJ11 of migmatitic biotite-gneisses fall in the field of shoshonite serie. Judging from the aluminum saturation index  $A/\text{CNK}$  (= molar  $\text{Al}_2\text{O}_3 / (\text{CaO} + \text{Na}_2\text{O} + \text{K}_2\text{O})$ ; [23]) in figure 4c, the amphibolites are metaluminous ( $A/\text{CNK} = 0.775-0.9$ ), whereas migmatitic biotite-gneisses and migmatitic mylonitic gneisses are slightly metaluminous to peraluminous ( $A/\text{CNK} = 0.92-1.08$ ), and all the analyzed rock samples conform to I-type rocks [24] with  $A/\text{CNK} \leq 1.1$ .

Major element variations for PM rocks are shown on selected graphs in figure 5. The three rock types form well-defined clusters and, taken together, define more or less well-defined trends, where the overall major element concentrations decrease monotonously with increasing amount of  $\text{SiO}_2$ , whereas  $\text{K}_2\text{O}$  concentrations increase with increasing  $\text{SiO}_2$  contents and the variation of  $\text{Na}_2\text{O}$  is independent of the silica values (Fig. 5). Amphibolites (2.21–6.72%  $\text{MgO}$ ) show some slight chemical differences with other samples, in particular their lower content of  $\text{K}_2\text{O}$  (2.44–3.82%) and their higher contents in  $\text{Fe}_2\text{O}_{3(\text{T})}$  (5.76–8.62%),  $\text{TiO}_2$  (0.56–1.42%),  $\text{CaO}$  (4.4–5.39%), and the average value of  $\text{Al}_2\text{O}_3$  is 15.07. The total alkali concentrations are uniform within each rock type, that is, 7.63–9.23% in migmatitic biotite-gneisses, 8.36–8.56% in migmatitic mylonitic gneisses, and 6.21–7.17% in amphibolites. The Penja migmatite rock types are K rich and show  $\text{Na}_2\text{O}/\text{K}_2\text{O}$  ratios ranging from 0.27 to 1.55, and displaying characteristics of High-K calc-alkaline to shoshonitic rocks. Compared to the diorites of [25], amphibolites differ with a weak enrichment in  $\text{CaO}$  and poverty in  $\text{K}_2\text{O}$ . Comparing with the andesites from the continental margin [26], they are slightly depleted in  $\text{SiO}_2$  and enriched in  $\text{Fe}_2\text{O}_3$ . Although The Penja migmatite rock types contain low contents of loss on ignition ( $\text{LOI} = 0.11-1.43\%$ ; Table 1), they could contain small measurable amounts of volatile materials such as  $\text{OH}$ ,  $\text{CO}_2$  and  $\text{H}_2\text{O}$ .

Trace element concentrations of the Penja migmatite rocks are listed in table 1. Selected elements are plotted against  $\text{SiO}_2$  content in figure 5. Ga, Nb, Rb, Sr, Y concentrations decrease whereas Th values increase with increasing  $\text{SiO}_2$  content. Ba and Zr contents are in general scattered on variation diagrams (Fig. 5). Ba/Sr and Ba/Rb ratios range between 0.9-4.63 and 0.76-11.08 respectively, whereas K/Rb ratios vary from 73.98 to 209.91. These values are similar to those observed in continental calc-alkaline igneous suites [27], [28]. Elements such as Zr (46-499 ppm), Zn (30-190 ppm) and Pb (14-52 ppm) are concentrated in the rocks while Hf (1.7-11.3 ppm), Ta (0.1-1.8 ppm), U (1-47.1 ppm), Rb/Sr (0.24-3.31) are depleted. The high contents of Ba (128-1750 ppm), Sr (67-669 ppm), Rb (158-341 ppm) and Nd (17.3-96.7 ppm) are related to the participation of crust during the genesis of these rocks. Y/Nb (0.75-3) ratios are similar to those of tholeiites [29] and distinctively higher contents of Th are observed in the samples (Table 1).

Total REE is higher in amphibolites ( $\Sigma\text{REE} = 138.68-552.45$  ppm) and migmatitic biotite-gneisses ( $\Sigma\text{REE} = 246.06-375.44$  ppm) compared to migmatitic mylonitic gneisses ( $\Sigma\text{REE} = 99.68-127.47$  ppm). Chondrite-normalized REE patterns (Fig. 4d) are parallel and resemble each other, they indicate LREE enrichment but variable LREE/HREE ratios ( $\text{La}_\text{N}/\text{Yb}_\text{N} = 5.11-61.5$ ). Migmatitic mylonitic gneisses and migmatitic biotite gneisses display consistent fractionation trends within the LREE and HREE groups ( $\text{La}_\text{N}/\text{Yb}_\text{N} = 22.9-61.5$ ;  $\text{La}_\text{N}/\text{Sm}_\text{N} = 3.49-6.43$ ;  $\text{Ce}_\text{N}/\text{Yb}_\text{N} = 20.3-45.55$ ;  $\text{Gd}_\text{N}/\text{Yb}_\text{N} = 2.16-5.39$ ). REE patterns of amphibolites are less fractionated ( $\text{La}_\text{N}/\text{Yb}_\text{N} = 5.11-47.59$ ;  $\text{Gd}_\text{N}/\text{Yb}_\text{N} = 1.25-3.87$ ;  $\text{Ce}_\text{N}/\text{Sm}_\text{N} = 2.13-4.42$ , Fig. 4d) than those of the other rock groups. Negative  $\text{Eu}^*$  anomalies are pronounced in migmatitic mylonitic gneisses ( $\text{Eu}/\text{Eu}^* = 0.26-0.35$ ) and migmatitic biotite-gneisses ( $\text{Eu}/\text{Eu}^* = 0.45-0.72$ ), whereas they are not significant in the amphibolites ( $\text{Eu}/\text{Eu}^* = 0.57-0.87$ ).

In the normalized multi-elements of spider diagram related to chondrite (Fig. 4e), all the rocks show a distinctive depletion of Nb, Ta, Sr, P, and Ti relative to other trace elements and characteristic of calc-alkaline granites of crustal origin [30]. Also, they are enriched with large-ion lithophile elements (LILE), and display negative anomalies in Ba; Nb, Ta, Sr, P, Ti and Y. Penja migmatite rocks display less pronounced negative anomalies in Nb, Sr and Zr, and lower in Y and Tm values resulting in more fractionated trace elements distribution patterns, characteristic of calcalkaline arc granitoids.

TABLE 1  
CHEMICAL COMPOSITION OF PENJA MIGMATITE ROCKS

	Migmatitic biotite-gneiss			Migmatitic mylonitic gneiss			Amphibolite						
	AS <sup>1</sup>	DL <sup>2</sup>	AM <sup>3</sup>	PJ11	PJ17	PJ18	PJ6	PJ7	PJ8	PJ2	PJ3	PJ4	PJ14
SiO <sub>2</sub> (%)	0.01	FUS-ICP	69.49	68.78	68.68	74.61	73.65	75.13	60.22	60.67	60.55	55.33	60.66
TiO <sub>2</sub>	0.001	FUS-ICP	0.44	0.502	0.529	0.115	0.074	0.05	1.404	1.367	1.42	0.631	0.562
Al <sub>2</sub> O <sub>3</sub>	0.01	FUS-ICP	14.65	14.45	14.51	13.09	12.96	13.65	14.85	14.49	15.49	15.58	14.94
Fe <sub>2</sub> O <sub>3</sub> (T) <sup>4</sup>	0.01	FUS-ICP	3.93	4.65	4.61	2.8	2.51	1.84	7.12	6.85	7.82	8.62	5.76
FeO* <sup>5</sup>		FUS-ICP	3.54	4.19	4.15	2.52	2.26	1.66	6.41	6.17	7.04	7.76	5.18
MgO	0.01	FUS-ICP	0.53	0.86	0.96	0.13	0.08	0.06	2.3	2.21	2.39	6.72	5.3
MnO	0.001	FUS-ICP	0.05	0.062	0.063	0.034	0.028	0.02	0.095	0.094	0.1	0.165	0.101
CaO	0.01	FUS-ICP	1.39	2.48	2.43	0.95	0.98	1.13	4.51	4.4	4.52	5.39	5.2
Na <sub>2</sub> O	0.01	FUS-ICP	2.76	3.44	3.29	3.27	3.23	3.68	3.46	3.4	3.33	3.7	3.77
K <sub>2</sub> O	0.01	FUS-ICP	6.47	4.38	4.34	5.29	5.29	4.68	3.71	3.71	3.82	3.04	2.44
P <sub>2</sub> O <sub>5</sub>	0.01	FUS-ICP	0.16	0.18	0.2	0.01	< 0.01	0.01	0.52	0.51	0.55	0.35	0.3
LOI <sup>6</sup>		GRAV	0.31	0.35	0.42	0.38	0.22	0.39	1.09	0.88	0.56	1.09	1.43
Total	0.01	FUS-ICP	100.2	100.1	100	100.7	99.04	100.6	99.28	98.58	100.6	100.6	100.5
Na <sub>2</sub> O+K <sub>2</sub> O			9.23	7.82	7.63	8.56	8.52	8.36	7.17	7.11	7.15	6.74	6.21
Na <sub>2</sub> O/K <sub>2</sub> O			0.43	0.79	0.76	0.62	0.61	0.79	0.93	0.92	0.87	1.22	1.55
Ag (ppm)	0.5	FUS-MS	1	0.9	0.8	< 0.5	< 0.5	< 0.5	1.6	1.6	1.7	< 0.5	< 0.5
As	5	FUS-MS	< 5	< 5	< 5	< 5	< 5	< 5	< 5	< 5	< 5	< 5	< 5
Ba	3	FUS-MS	1080	1200	1370	171	159	128	1750	1750	1740	372	690
Be	1	FUS-ICP	2	5	4	3	2	3	3	3	3	7	4
Bi	0.4	FUS-MS	< 0.4	< 0.4	< 0.4	< 0.4	< 0.4	< 0.4	< 0.4	< 0.4	< 0.4	< 0.4	< 0.4
Co	1	FUS-MS	5	7	7	< 1	1	1	17	16	18	30	25
Cr	20	FUS-MS	< 20	< 20	< 20	< 20	< 20	< 20	50	50	60	340	290
Cs	0.5	FUS-MS	2.8	4	4.4	2.4	1.8	1.2	2.9	3.6	3.2	11.4	8.3
Cu	10	FUS-MS	10	130	70	50	20	< 10	20	20	30	< 10	< 10
Ga	1	FUS-MS	22	21	20	21	20	20	22	22	24	24	21
Ge	1	FUS-MS	1	1	1	< 1	< 1	1	1	1	1	2	2
Hf	0.2	FUS-MS	7.9	6.3	5.8	2.3	1.7	3	11	11.3	11.2	2.1	2.6
In	0.2	FUS-MS	< 0.2	< 0.2	< 0.2	< 0.2	< 0.2	< 0.2	< 0.2	< 0.2	< 0.2	0.2	< 0.2
Mo	2	FUS-MS	2	> 100	11	< 2	< 2	< 2	2	2	3	4	< 2
Nb	1	FUS-MS	17	16	15	6	3	3	29	30	32	25	16
Ni	20	FUS-MS	< 20	< 20	< 20	< 20	< 20	< 20	20	< 20	< 20	130	100
Pb	5	FUS-MS	38	23	23	52	52	49	22	24	24	14	17
Rb	2	FUS-MS	257	188	197	225	215	185	158	174	167	341	269
Sb	0.5	FUS-MS	< 0.5	< 0.5	< 0.5	< 0.5	< 0.5	< 0.5	< 0.5	< 0.5	< 0.5	< 0.5	< 0.5
Sc	1	FUS-ICP	3	3	3	2	1	< 1	11	11	12	16	12

<sup>1</sup> Analyte symbol; <sup>2</sup> Detection limit; <sup>3</sup> Analysis method; <sup>4</sup> Total iron; <sup>5</sup> FeO\* = 0.9Fe<sub>2</sub>O<sub>3</sub>(T); <sup>6</sup> Loss on ignition



TABLE 1  
 CONTINUED

Sn	1	FUS-MS	2	4	3	2	2	1	3	3	3	9	5
Sr	2	FUS-MS	242	496	464	68	67	69	663	650	669	412	497
Ta	0,1	FUS-MS	0.7	1.7	1.5	0.2	< 0.1	< 0.1	1.7	1.8	1.8	1.8	1.4
Th	0,1	FUS-MS	58.9	18.8	22.6	26.8	20.6	23.3	24.4	25.3	25.1	4.1	9
Tl	0,1	FUS-MS	1.1	1	1	1	1	0.8	0.7	0.9	0.9	1.8	1.5
U	0,1	FUS-MS	7.9	4.7	6.1	47.1	39.1	26.1	3.2	3.3	3.2	1	7.5
V	5	FUS-MS	27	46	50	5	< 5	< 5	92	91	97	103	87
W	1	FUS-MS	< 1	2	< 1	< 1	< 1	< 1	< 1	< 1	< 1	< 1	< 1
Y	1	FUS-MS	14	18	16	9	7	9	24	24	24	35	19
Zn	30	FUS-MS	60	60	70	30	< 30	< 30	120	120	130	190	90
Zr	5	FUS-MS	296	237	219	60	46	73	499	493	490	72	88
Ba/Sr			4.46	2.42	2.95	2.51	2.37	1.86	2.64	2.69	2.60	0.90	1.39
Ba/Rb			4.20	6.38	6.95	0.76	0.74	0.69	11.08	10.06	10.42	1.09	2.57
Rb/Sr			1.06	0.38	0.42	3.31	3.21	2.68	0.24	0.27	0.25	0.83	0.54
Y/Nb			0.82	1.13	1.07	1.50	2.33	3.00	0.83	0.80	0.75	1.40	1.19
K/Rb			208.90	193.32	182.81	195.09	204.17	209.91	194.84	176.93	189.81	73.98	75.27
Ce/Pb			4.63	4.87	5.04	1.09	0.83	1.12	11.50	10.71	10.75	3.53	3.15
La (ppm)	0,1	FUS-MS	91.1	61.3	64.3	27.2	22.7	27.9	131	137	141	26.5	28.4
Ce	0,1	FUS-MS	176	112	116	56.8	43.3	54.9	253	257	258	49.4	53.5
Pr	0,05	FUS-MS	20.1	11.8	12.1	6.69	5.02	6.27	27.3	27.8	28.5	5.93	6.46
Nd	0,1	FUS-MS	64.5	39.5	39.5	22.5	17.3	21.1	93.2	92.1	96.7	22.6	24.3
Sm	0,1	FUS-MS	9.9	6.7	6.3	4.9	4.1	4.7	13.9	14.1	14.1	5.6	5
Eu	0,05	FUS-MS	1.13	1.32	1.26	0,38	0,4	0,4	2.75	2.77	2.94	1.03	1.34
Gd	0,1	FUS-MS	5.9	4.8	4.6	4	3	3.5	9.1	9.3	9.4	5.4	4.6
Tb	0,1	FUS-MS	0.7	0.6	0.6	0.5	0.4	0.4	1.1	1.1	1.1	0.9	0.6
Dy	0,1	FUS-MS	2.9	3.4	3.1	2.4	1.8	2.3	5.4	5.4	5.5	5.5	3.1
Ho	0,1	FUS-MS	0.5	0.6	0.6	0.4	0.3	0.3	0.9	0.9	0.9	1.1	0.6
Er	0,1	FUS-MS	1.4	1.7	1.5	0.9	0.7	0.9	2.5	2.4	2.3	3.2	1.5
Tm	0,05	FUS-MS	0.17	0.27	0.23	0.11	0.09	0.11	0.31	0.31	0.3	0.49	0.23
Yb	0,1	FUS-MS	1	1.8	1.6	0.6	0.5	0.7	1.9	2	2	3.5	1.6
Lu	0,01	FUS-MS	0.14	0.27	0.25	0.09	0.07	0.1	0.29	0.27	0.29	0.53	0.25
ΣREE			375.44	246.06	251.94	127.47	99.68	123.58	542.65	552.45	563.03	131.7	251.94
(La/Yb)N			61.49	22.99	27.13	30.60	30.64	26.90	46.54	46.24	47.59	5.11	27.13
(Gd/Yb)N			4.77	2.16	2.32	5.39	4.85	4.04	3.87	3.76	3.80	1.25	2.32
(Ce/Sm)N			4.29	4.04	4.45	2.80	2.55	2.82	4.39	4.40	4.42	2.13	4.45
(Ce/Yb)N			45.55	16.10	18.76	24.50	22.41	20.30	34.46	33.26	33.39	3.65	18.76
(La/Sm)N			5.79	5.76	6.43	3.49	3.49	3.74	5.93	6.12	6.30	2.98	6.43
Eu/Eu*			0.45	0.71	0.72	0.26	0.35	0.30	0.75	0.74	0.78	0.57	0.72

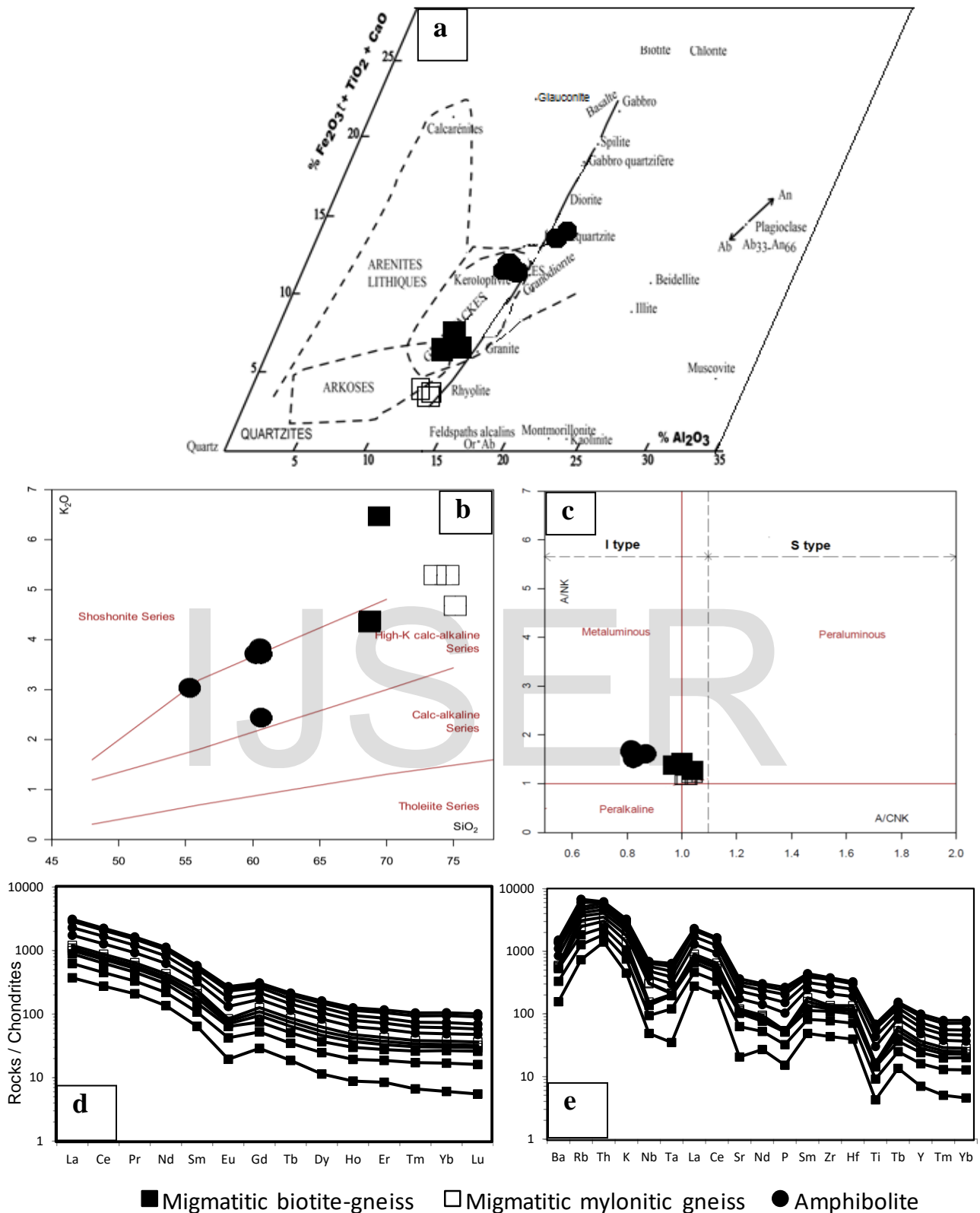


**Fig. 4:** (a)  $\text{Fe}_2\text{O}_3 + \text{TiO}_2 + \text{CaO}$  against  $\text{Al}_2\text{O}_3$  plot showing the whole rock chemical composition of Penja migmatite rocks. (b)  $\text{SiO}_2$ - $\text{K}_2\text{O}$  plot showing High-K calc-alkaline affinity; (c) alumina index diagram (molar  $\text{Al}_2\text{O}_3 / (\text{CaO} + \text{Na}_2\text{O} + \text{K}_2\text{O})$  vs  $\text{Al}_2\text{O}_3 / (\text{Na}_2\text{O} + \text{K}_2\text{O})$ ); (d) REE pattern (normalizations values as from [31] and (e) spider diagram (normalizing values are according to [32]).

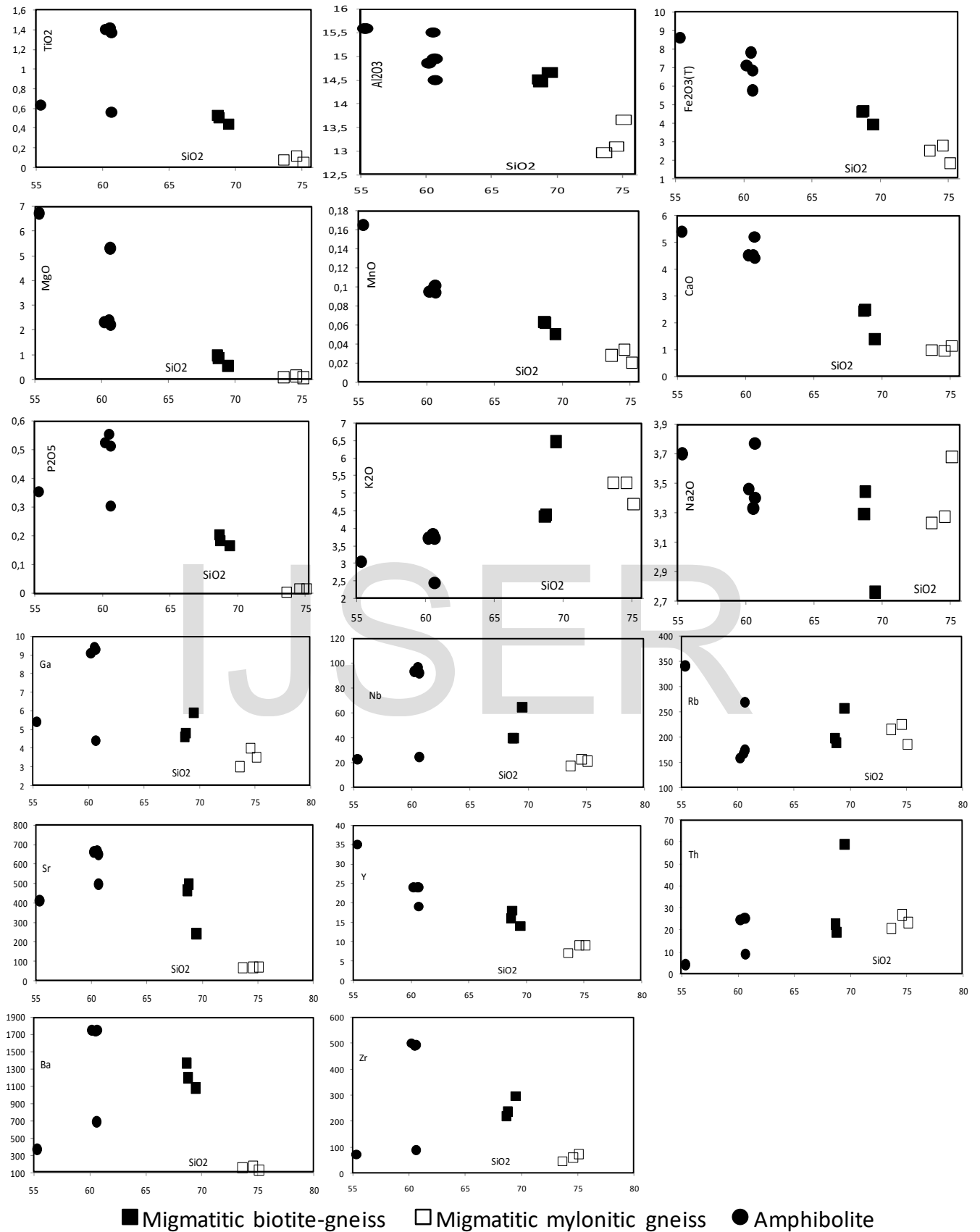


Fig. 5: Selected Harker diagrams of major and trace elements for PMs

## 5 DISCUSSION

The most common metamorphic lithology in Penja is migmatitic gneiss whose migmatitic biotite-gneiss represents the dominant rock type. Field observations and petrography results favour a melting process. Anatexis or subsolidus differentiation is the usual question arising in any migmatite study [5], [33] - [35]. Anatexis of naturally occurring rocks is very complex and is greatly influenced by protolith composition and the temperature of melting [36] - [38]. In the study area, migmatitic gneisses range from metatexites to diatexite [3], [39] related to the amphibolites facies. The metatexite is underlined on the field by a pervasive foliation, the proportion of neosome varies between 20 to 50% and it segregated into leucosome and melanosome, the paleosome consists of amphibolite. The diatexite is underlined by various appearances of neosome such as the variation of textures, compositions of neosome and the disappearance of pre-migmatite structures. The PMs fall into the group of gneissic granitic rock according to [3] terminology.

In the Penja migmatites, the quartzo-feldspathic fraction and related ferromagnesian minerals are frequently associated although dark selvages are seldomly observed; they are best referred to as neosomes after [40]. Penja migmatitic gneisses experienced three types of neosome: leucosome, melanosome and mesosome. This is interpreted as the result of incipient migmatization of the gneiss. The presence of neosome suggests after [41] a high rheological contrast between neosomes and the surrounding gneiss. Migmatitic gneisses are also reported in Olkiluoto [39] and in the Yaoundé Serie by [9], [15], [42]), and in the Nyong Serie [41] and their neosome have similarities with the Penja migmatite neosome. Furthermore, in the study area, the neosome and mesosome have a layered structure and can be classified according to the migmatitic structure as stromatic after [6] and [39].

According to [5] terminology, three types of leucosomes have been recognized in the study area: leucosome dike, in situ leucosome and in-source leucosome. The in situ leucosomes result from the partial melting in disequilibrium. They have been segregated from the parent and remained at the place of melting. The In-source leucosomes have moved from the melting place and remained in the source unit. Leucocratic dikes result from the partial melting near the equilibrium of fractionated crystallization of anatectic liquids. They have migrated out from its protolith and remained in the same environment which went through the partial melting. Furthermore, the difference between the three types of leucosomes could be linked to the difference in the composition of their source and the probable contamination during transportation of the melting material [15]. These three types of leucosome are also reported by [3] in Olkiluoto whereas [15] and [42] recorded in the Yaoundé Series two types of leucosome: injection leuco-

somes and in situ leucosomes. The partial melting constitutes the mechanism in the formation of PM and therefore the migmatitic rocks of Penja refer after [43] and [44] to venite.

The nature of protoliths can be constrained using the geochemical signatures of the rocks. The behavior of Penja migmatite rocks on Harker diagrams does not indicate a continuous compositional variation, but clearly expresses three distinct groups; this reveals that the chemical differences of these rocks seem to reflect the primary compositions of three distinct source rocks. Therefore, the plot of the samples in figure 5 defines a chemical trend parallel to the igneous rocks origin, and the Penja migmatites derive from three protoliths: granite, granodiorite and diorite quartzite. They yield intermediate to acid rocks according to the classification of [45] based on silica concentration in the rock analysis. The investigated metamorphic rocks exhibit petrographical and chemical compositions characteristic of High-K calc-alkaline series and I-type rocks [24] and [46]. High-K calc-alkaline suites are also reported by [47] for the Ngaoundéré granitoids. K-rich rocks are generally derived from the partial melting of metamorphosed hydrous intermediate calc-alkaline rocks [48]. The fact that the studied rocks have high alkali contents (6.21–9.23%) suggests that the Penja leucosomes could be enriched in alkali (K, Na) and to a lesser extent calc-alkali element (plagioclase could more Na-rich than Ca-rich), and can also contain appreciable amounts of Al and Si. This is in agreement with [36] stipulating that typical leucosomes are generally leucogranitic to trondhjemitic or granodioritic to tonalitic, depending on the starting material.

High SiO<sub>2</sub> (55.33-75.13%), Al<sub>2</sub>O<sub>3</sub> (12.93-15.58%) and low MgO (0.06-6.72%) coupled with the values of Ba/Sr (0.9-4.63), Ba/Rb (0.76-11.08), and Ce/Pb (0.83-11.71; average = 5.2) ratios, which are far from the typical mantle values (Ce/Pb = 25; [49]) suggest the participation of the crust [30] during the genesis of the penja migmatites; but distinctively higher contents of Th (4-58.9 ppm) are observed in the samples. Also, the overall enrichment in the incompatible elements (K, Rb, Ba) and depletion in high field strength elements (HFSE) supports the importance of the crustal source component in the genesis of these rocks. Sr (67-497 ppm) and Rb (158-341 ppm) are relatively high and the marked enrichment suggests their association with feldspar (Sr enters to feldspar structures and Rb is placed in the potassium feldspar structure). Sr and Ba are found in the same vertical column of the periodic table and are chemically alike. These are lithophile elements, very compatible and they strongly partition into feldspar. Sr has an ionic radius of 1.12Å and lies between Ca and K whose ionic radii are respectively 0.99Å and 1.33Å. Sr is therefore expected to substitute for both elements in the rock due to the proximity of their ionic radii.

The relatively low Rb/Sr (0.24-4.42) and the LREE-enriched could be related to the enrichment of their source materials.

According to [50] concentration of LREE is the unique specification of Ocean-Island Basalt (OIB) which shows presence of residual garnet in the source. The presence of Th and Pb in the rocks reflects their mutual association as large-ion lithophile elements (LILE) that are usually mobile and radioactive.

Chondrite-normalized REE patterns (Fig. 4d) for Penja migmatites indicate LREE enrichment ( $La_N/Yb_N = 5.11-61.5$ ) compared to HREE ( $Gd_N/Yb_N = 1.25-5.39$ ). The LREE enrichment and HREE depletion behavior had also been noticed by [12], [51] and interpreted as compatible with fractionation of amphibole which tends to concentrate the HREE. Enriched incompatible elements of LREE and depleted HREE in the presence of volatile materials in the opinion of [52], [53] are characteristics of rocks that are of mantle sources. REE spectrum show mostly weakly negative Eu anomalies ( $Eu/Eu^* = 0.26-0.87$ ; Figs. 4d, 6), which can be attributed to the partial melting [54]. Eu anomalies are often controlled by feldspars since Eu is stable in its bivalency in calcium feldspars; while, other trivalent REE are inconsistent in calcium feldspars. Therefore, separating calcium feldspar from the melting phase can lead to a negative anomaly of Eu either the separation has been caused by crystalline separation or partial separation [50]. The Eu depletion is probably because of plagioclase removal from the source or later discarding by fractional crystallization in the magma chamber prior to emplacement [55]. Based on the theory raised by [56], negative anomaly of Ba, Sr, P, and Ti (Fig. 4e) shows fractional crystallization.

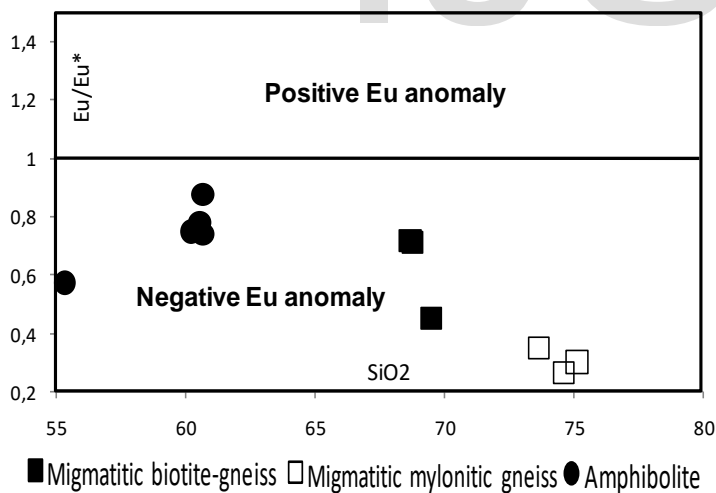


Fig. 6: Diagram of  $Eu/Eu^*$  versus  $SiO_2$  [57] displaying negative Eu anomalies for Penja migmatites.

## 6 CONCLUSION

The Penja migmatites (PMs) within the central domain of the Pan-African fold belt in Cameroon outcrop as a large body of migmatitic gneiss comprising migmatitic biotite-gneisses as

major rock types, migmatitic mylonitic gneisses, amphibolites and granite pegmatites. Field observations and petrography results favour a melting process and Penja migmatites range from metatexites to diatexite related to the amphibolites facies. The Penja migmatitic gneisses display three types of neosome notable leucosome, melanosome and mesosome. This is interpreted as the result of incipient migmatization of the gneiss. The presence of neosome suggests a high rheological contrast between the neosomes and the surrounding gneiss. The proportion of neosome varies between 20 to 50% and it segregated into leucosome and melanosome; the PMs neosome has similarities with the neosome recorded in the Yaoundé Serie and Nyong Serie. The PMs fall into the group of gneissic granitic rock; stromatic structures and granoblastic microstructures prevail in the rock types, but mylonitic microstructures are also frequently observed.

Three types of leucosome have been recognized in the PMs. They include leucosome dike, in situ leucosome and in-source leucosome and the difference between the three types could be linked to the difference in the composition of their source and the probable contamination during transportation of the melting material. These three types of leucosome are also recorded in Olkiluoto, whereas injection leucosomes and in situ leucosomes have been reported in the Yaoundé Series. The partial melting constitutes the mechanism in the formation of PMs and therefore the migmatite rocks from Penja refer to venite.

PM rocks exhibit the composition of intermediate to acid High-K calc-alkaline series and I-type rocks derived from continental igneous protoliths varying from granite to diorite quartzite through granodiorite. The REE and multi-element patterns are in accordance with genetic processes involving participation of the crust. In addition, REE spectrums show weakly negative Eu anomalies which are attributed to the partial melting.

## REFERENCES

- [1] J. Sederholm, "On granite and gneiss," Bull. Comm. Géol. Finlande. p23, 1907
- [2] K. Mehnert, Migmatite and origin of granitic rocks. Elsevier, Amsterdam: p393, 1968.
- [3] A. Kärti, "Migmatite and migmatite-like rocks of Olkiluoto," Working reports 2015-03. Posiva Oy, EURAJOKI, Finland. p61, 2015.
- [4] W. Wimmenauer, and I. Bryhni, "Towards a unified nomenclature of metamorphic petrology: migmatites and related rocks. A proposal on behalf of the IUGS Subcommittee on the Systematic of Metamorphic Rocks," Web-version 31.07.2002. [www.bgs.ac.uk/SCMR/paper\\_7/scmr\\_paper\\_07.pdf](http://www.bgs.ac.uk/SCMR/paper_7/scmr_paper_07.pdf). p7.
- [5] E.W. Sawyer, "Atlas of migmatites," The Can. Miner. Spec. Publ. 9, NRC Research Press, Ottawa, Ontario, Canada, p 371, 2008.
- [6] S. Robertson, "BGS Rock classification scheme," Volume 2: Classification of metamorphic rocks. British Geology Survey Research Report, RR 99-02, p24, 1999.
- [7] C. Castaing, J.L. Feybesse, D. Thieblemont, C. Triboulet, & P. Chevremont, "Palaeogeographical reconstructions of the Pan-

- African/Brasiliano orogen: closure of an oceanic domain or intracontinental convergence between major blocks," *Prec Res.* Vol. 69, pp. 327-344, 1994.
- [8] S.P. Neves, J.M.R. Silva, & G. Mariano, "Oblique lineations in orthogneisses and supracrustal rocks: vertical partitioning of strain in a hot crust (eastern Borborema Province, NE Brazil)," *J. Struct Geol.* Vol. 27, pp. 1507-1521, 2005.
- [9] J.P. Nzenti, P. Barbey, J. Macaudiere and D. Soba, "Origin and evolution of the late Precambrian high-grade Yaounde gneisses (Cameroon)," *Prec Res.* Vol. pp. 38, 91-109, 1988.
- [10] J.P. Nzenti, P. Barbey, J.M.L. Bertrand et J. Macaudière, "La chaîne panafricaine au Cameroun: cherchons suture et modèle," In S.G.F. édit, 15e réunion des Sciences de la Terre, Nancy, France, p 99, 1994.
- [11] J.P. Nzenti, P. Barbey, F.M. Tchoua, "Evolution crustale au Cameroun éléments pour un modèle géodynamique de l'orogénèse néoproterozoïque," In *Géologie et environnements au Cameroun*, Vicat et Bilong eds, collection GEOCAM 2, pp. 397-407, 1999.
- [12] J.P. Nzenti, B. Kapajika, G. Wörner and R.T. Lubala, "Synkinematic emplacement of granitoids in a Pan-African shear zone in Central Cameroon," *J. Afr. Earth Sci.* Vol. 45, pp. 74-86, 2006.
- [13] E.L. Tanko Njiosseu, "Géologie de la région de Tonga dans la partie Sud du domaine centre de la chaîne au Cameroun: évolution métamorphique, géochimie et géochronologie," Thèse de Doctorat PhD, Dept des Sciences de la Terre, Univ. de Yaoundé I, 2012.
- [14] T. Ngnotué, J.P. Nzenti, P. Barbey, and F.M. Tchoua, "The Ntui-Betamba high-grade gneisses: a Northward extension of the Pan-African Yaounde gneisses in Cameroon," *J. Afr. Earth Sci.* Vol. 31, pp. 369-381, 2000.
- [15] T. Ngnotué, S. Ganno, J.P. Nzenti, B. Schulz, D. Tchaptchet Tchato, E. Suh Cheo, "Geochemistry and geochronology of Peraluminous High-K granitic leucosomes of Yaoundé series (Cameroon): evidence for a unique Pan-African magmatism and melting event in North Equatorial Fold Belt," *Int. J. Geosci.* Vol. 3, pp. 525-548, 2012.
- [16] S.F. Toteu, W.R. Van Schmus, J. Penaye, A. Michard, "New U-Pb and Sm-Nd data from North-Central Cameroon and its bearing on the pre-pan African history of Central Africa" *Pre Res.* Vol. 108, pp. 45-73, 2001.
- [17] B. Kankeu, R.O. Greiling, J.P. Nzenti, "Pan-African strike-slip tectonics in eastern Cameroon-Magnetic fabrics (AMS) and structure in the Lom basin and its gneissic basement (Bétare-Oya area)," *Prec. Res.* Vol. 17, no. 3-4, pp. 258-272, 2009.
- [18] B., Kankeu, R.O. Greiling, J.P. Nzenti, S. Ganno, P.Y.E. Danguene, J. Bassahak, J.V. Hell, "Contrasting Pan-African structural styles at the NW margin of the Congo Shield in Cameroon," *J. Afr. Earth Sci.* <http://dx.doi.org/10.1016/j.jafrearsci.2017.06.002>.
- [19] J.P. Nzenti, Neoproterozoic alkaline metamorphic igneous rocks from the Pan-african North Equatorial fold belt (Yaounde, Cameroon): biotites and magnetite rich pyroxenites. *J. Afr. Earth Sci.* Vol. 26, no. 1, pp 37-47, 1998.
- [20] J. Siivola and R. Schmid, "List of Mineral Abbreviations. Recommendations by the IUGS Subcommittee on the Systematics of Metamorphic Rocks," Web version 01.02.2007; [www.bgs.ac.uk.scmr/home.html](http://www.bgs.ac.uk.scmr/home.html).
- [21] H. De la Roche, "Sur l'existence de plusieurs faciès géochimiques dans les schistes paléozoïques des Pyrénées lychonnaises," *Geol. Rundsch.* Vol. 55, pp. 274-301, 1965.
- [22] A. Peccerillo, & S.R. Taylor, "Geochemistry of Eocene calc-alkaline volcanic rocks from the Kastamonu area, Northern Turkey". *Contrib. Mineral. Petrol.* Vol. 58, pp. 63-81, 1976.
- [23] S.J. Shand, *The eruptive rocks.* Second ed. John Wiley, New York, p444, 1943.
- [24] B.W. Chappell, A.J.R. "White, I- and S-type granites in the Lachlan Fold Belt," *Trans. Royal Soc. Edinburgh Earth Sci.*, Vol. 83, no. 1, 1-12, 1992.
- [25] R.W. Le Maître, *The Chemical Variability of some common igneous rocks.* *J. Petrol.* Vol. 17, pp. 589-637, 1976.
- [26] J.M. Bertrand, C. Dupuy, J. Dostal and I. Davidson, "Geochemistry and geotectonic interpretation of granitoids from Central Iforas (Mali, West Africa)," *Prec Res.* Vol. 26, no. 3-4, pp. 265-283, 1984.
- [27] A.R. McBirney, "Geology and petrology of the Galagos Island," *Boulder, Colloquium /Geological Society of America.* p 197, 1969.
- [28] R. Ayuso, and J.G. Arth, "The Northeast Kingdom batholith, Vermont: magmatic evolution and geochemical constraints on the origin of Acadian granitic rocks," *Contrib. Mineral. Petrol.* Vol. 111, no. 1, pp. 1-23, 1992.
- [29] J.A. Pearce, and J.R. Cann, 1973 "Tectonic setting of basic volcanic rocks determined using trace element analyses," *Earth Planet. Sci. Lett.* Vol. 19, pp. 290-300, 1973.
- [30] R.N. Thompson, M.A. Morrisson, G.L. Hendry, and S.J. Parry, "An assessment of the relative role of crust and mantle in magma genesis. An element approach," *Philos. Trans. Royal. Soc. London.* Vol. 310, pp. 549-590, 1984.
- [31] N.M. Evensen, P.J. Hamilton, and R.K. O'Nions, "Rare earth abundances in chondritic meteorites," *Geochim. Cosmochim. Acta.* Vol 4, pp. 1199-1212, 1978.
- [32] R. N. Thompson, "Magmatism of the British Tertiary Volcanic Province," *Scot J. Geol.* Vol. 18, pp. 49-107, 1982.
- [33] E.W. Sawyer, and S.J. Barnes, "Temporal and compositional differences between subsolidus and anatectic migmatite leucosomes from the Quetico metasedimentary belt, Canada," *J. Metam. Geol.* Vol. 6 no. 4, pp. 437-450, 1988.
- [34] E.L. McLellan, "Sequential formation of subsolidus and anatectic migmatites in to thermal evolution, eastern Scotland," *J. Geol.* Vol. 97, pp. 165-182, 1989.
- [35] R.O. Maxeiner, K. Ashton, C.D. Card, R.M. Morelli, and B. Knox, "A field guide to naming migmatites and their textures, with Saskatchewan examples; in Summary of Investigations" Saskatchewan Geological Survey, Saskatchewan Ministry of the Economy, Miscellaneous Report 2017-4.2, Paper A-2, p21, 2017.
- [36] H.G.F. Winkler, 1979, "Petrogenesis of Metamorphic Rocks," 5th Edition; Springer-Verlag: New York Inc., p348, 1979.
- [37] Yardley, B.W.D., 1989. "An Introduction to Metamorphic Petrology," Longman Scientific & Technical, Essex, England, 248p.
- [38] E.W. Sawyer, and M. Brown, "Working with migmatites," *Mineralogical Association of Canada, Short Course Vol. 38,* 158p, 2008.
- [39] J. Mattila, "A system of nomenclature for rocks in Olkiluoto," *Working reports 2006-32.* Posiva Oy, EURAJOKI, Finland. p26, 2006.
- [40] J.R. Ashworth, "Migmatites," Blackie, USA: Chapman & G. Hall. New York, 1985.
- [41] A. Nédélec, D. Minyem, and P. Barbey, "High-P high-T anatexis or archaean tonalitic grey gneisses: the Eseké migmatites, Cameroon," *Prec Res.* Vol. 62, pp. 191-205, 1993.
- [42] J.P. Nzenti, "Pétrogénèse des migmatites de Yaoundé (Cameroun): éléments pour un modèle géodynamique de la Chaîne Panafricaine Nord-Equatoriale," Thèse de Doctorat, Univ. Nancy I, 1987.
- [43] P. Holmquist, "Swedish Archaean structures and their meaning". *Bull. Geol. Inst. Uppsala.* Vol. 15, pp. 125-148, 1916.
- [44] R.W. Le Maitre, eds, P. Bateman, A. Dudek J. Keller, et al "A Classification of Igneous rocks and Glossary of Term: Recommendations of the International Union of Geological Sciences Subcommittee on the Systematics of Igneous Rocks," Blackwell Scientific Publications, Oxford, 1989.

- [45] B.W. Chappell, and A.J.R. White, "Two contrasting granite types," *Pacific Geology*. Vol. 8, pp. 173-174, 1974.
- [46] R. Tchameni, A. Pouclet, J. Penaye, A.A. Ganwa, and S.F. Toteu, "Petrography and geochemistry of the Ngaoundéré Pan-African granitoids in Central North Cameroon: Implications for their sources and geological setting," *J. Afr. Earth Sci.* Vol. 44, pp. 511-529, 2006.
- [47] M.P Roberts, J.D. Clemens, "Origin of high-potassium, calcalkaline, I-type granitoids," *Geology* Vol. 21, no. 9, pp. 825-828, 1993.
- [48] A.W. Hofmann, K.P. Jochum, M. Seufert, W.M. White, "Nb and Pb in oceanic basalts: new constraints on mantle evolution," *Earth Planet. Sci. Lett.* Vol. 79, pp. 33-45, 1986.
- [49] E. Nazemi, A.A. Mohammad, J. Abdoreza, P. Mohsen, "Petrology and Geochemistry of Igneous Rocks in Zarinkamar Area, NE of Shahrood, Iran," *Open J. Geol.* Vol. 7, pp. 348-359, 2017.
- [50] G.D. Kouankap Nono, P. Wotchoko, A. Magha, S. Ganno, N. Njoya, A. Afahwile Ngambu, J.P. Nzenti, V. Kamgang Kabeyene, "Contrasting Ba-Sr Granitoids from Bamenda Area, NW Cameroon: Sources Characteristics and Implications for the Evolution of the Pan African Fold Belt," *J. Geosci. Geom.* Vol. 6, no. 2, pp. 65-76, 2018.
- [51] D.A. Wood, J.L. Joron, and M. Treuil, "A reappraisal of the use of trace elements to classify and discriminate between magma series erupted in different tectonic settings," *Earth Planet. Sci. Lett.* Vol. 45, pp. 326-336, 1979.
- [52] J.A. Pearce, "Trace element characteristics of lava from destructive plate boundaries. In Thorpe R.S, eds *Andesites*," New York John Wiley and sons. 525-548, 1982.
- [53] Y. Teraokado, & A. Masuda, "Trace element variations in acidic rocks from the inner zone of southwest Japan," *Chem. Geol.* 67, 227-241, 1988.
- [54] S.M. Niktabar et al, "Petrogenesis of the Lalezargranitoid Intrusions (Kerman Province-Iran)," *J. Sci., Islamic Republic of Iran*, Vol. 26, pp. 333-348, 2015.
- [55] X.H. Li, H.W. Zhou, Y. Liu, C.Y. Lee, Sun, M. and C.H. Chen, "Shoshonitic Intrusive Suite in SE Guangxi: Petrology and Geochemistry," *Chin Sci Bull.* Vol. 45, pp. 653-659, 2000.
- [56] J.B. Brady, and J.T. Cheney, "The Cape Ann Plutonic Suite: A Field Trip for Petrology Classes," In: Hanson, L.S., Ed., *Guidebook to Field Trips from Boston, MA to Saco Bay, ME*, New England Intercollegiate Geological Conference, 96th Annual Meeting, Salem, Massachusetts. B5, pp. 1-26, 2004.
- [57] D. Fettes and J. Desmons- Metamorphic rocks: A classification and glossary of terms. Recommendations of the International Union of Geological Sciences Subcommission on the Systematics of Metamorphic Rocks. Cambridge University Press, 2007; 978-0-521-86810-5. p.190. [www.bgs.ac.uk/scmr/home.html](http://www.bgs.ac.uk/scmr/home.html)